



Discontinuities in hygroscopic growth below and above water saturation for laboratory surrogates of oligomers in organic atmospheric aerosols

5 Natasha Hodas,^{1,2} Andreas Zuend,³ Katherine Schilling,^{1,a} Thomas Berkemeier,⁴ Manabu Shiraiwa,⁴ Richard C. Flagan,^{1,5} John H. Seinfeld^{1,5}

¹Division of Chemistry and Chemical Engineering, California Institute of Technology, Pasadena, CA, USA

²Department of Environmental Sciences and Management, Portland State University, Portland, OR, USA

10 ³Department of Atmospheric and Oceanic Sciences, McGill University, Montreal, Quebec, Canada

⁴Multiphase Chemistry Department, Max Planck Institute for Chemistry, Mainz, Germany

⁵Division of Engineering and Applied Science, California Institute of Technology, Pasadena, CA, USA

^anow at: United States Army Criminal Investigation Laboratory, Forest Park, GA, USA

15 *Correspondence to:* Natasha Hodas (nhodas@pdx.edu)

Abstract. Organic oligomers and other organic high molecular mass compounds are potential sources of viscous atmospheric aerosol components, which may inhibit the mass transport of water and introduce kinetic limitations to water uptake. This, in turn, impacts aerosol optical properties and the efficiency with which these particles serve as cloud condensation nuclei (CCN). To investigate the influence of particle viscosity on water-uptake behavior, measurements of hygroscopic growth under subsaturated relative humidity (RH) conditions and of the CCN activity of laboratory surrogates for oligomers in atmospheric aerosols were conducted with the Differential Aerosol Sizing and Hygroscopicity Spectrometer Probe and a CCN counter, respectively. In order to explore variability in water-uptake behavior across aerosol systems with differing viscosities, experiments were conducted for particles comprised of polyethylene glycol (PEG) with average molecular masses of 200, 1,000, and 10,000 g/mol, as well as mixtures of these PEG oligomers with ammonium sulfate (AS). Experimental results were compared with calculations of hygroscopic growth at thermodynamic equilibrium conducted with the Aerosol Inorganic Organic Mixtures Functional groups Activity Coefficients (AIOMFAC) model, and the potential influence of kinetic limitations to observed water uptake was further explored through estimations of water diffusivity in the PEG oligomers. Under subsaturated RH conditions, we observed little variability in hygroscopic growth across PEG systems with different molecular masses; however, an increase in CCN activity with increasing PEG molecular mass was observed. This latter finding is attributed to an increase in the efficiency of PEG as a surfactant with increasing molecular mass. This effect is most pronounced for PEG-AS mixtures, and a modest enhancement in CCN activity was observed for the PEG10,000-AS mixture as compared to pure AS, as evidenced by a 8% reduction in critical activation diameter at a supersaturation of 0.6%. The supplementation of experimental observations with the AIOMFAC-based model results and estimations of water diffusivity in PEG suggests that apparent discontinuities in hygroscopicity above and below water saturation can be attributed, at least in part, to a combination of RH-dependent differences in the sensitivity of water uptake behavior to non-ideal interactions and to surface tension effects. There was no evidence that kinetic limitations to water uptake due to the presence of viscous aerosol components influenced



hygroscopic growth. This work provides insight into the factors likely to be contributing to discontinuities in aerosol water-uptake behavior below and above water saturation (e.g., low hygroscopic growth at subsaturated RHs, but enhanced CCN activity for a given aerosol population) that have been observed previously in the ambient atmosphere.

5

1 Introduction

The extent to which interactions between airborne aerosols and water vapor modulate the Earth's radiation budget is a source of uncertainty in projections of the impact of aerosols on radiative forcing (Boucher et al., 2013). The uptake of water in relative humidity (RH) regimes below water saturation ($RH < 100\%$) affects aerosol particle size distributions and optical properties, impacting the efficiency of scattering and absorption of solar radiation. Under supersaturated RH conditions relevant to the activation of cloud condensation nuclei (CCN), aerosol properties influence cloud droplet number, cloud albedo, and, potentially, cloud lifetime. Further, condensed-phase water present in atmospheric aerosols and cloud droplets serves as a medium into which reactive organic gases can partition and undergo aqueous-phase chemistry to form secondary organic aerosol (SOA) (McNeill, 2015 and references therein). While the water-uptake behavior of inorganic aerosol components is generally well characterized (Seinfeld and Pandis, 2006), a more thorough understanding of the influence of organic compounds on aerosol hygroscopicity and CCN activity is needed.

20 A complicating factor in the understanding and representation of the water-uptake behavior of organic and mixed organic-inorganic aerosols is the fact that such particles can exist in a variety of phase states. Non-ideal thermodynamic interactions between organic and inorganic particle components can result in liquid-liquid phase separation (LLPS) in which inorganic-dominated and organic-dominated phases coexist (Erdakos and Pankow, 2004; Ciobanu et al., 2009; Zuend et al., 2010; Bertram et al., 2011; Pöhlker et al., 2012; Song et al., 2012; Zuend and Seinfeld, 2012; You et al., 2012, 2013, 2014). Moreover, organic aerosol components can exist as viscous liquids, semisolids, and glasses depending on their composition and ambient conditions (e.g., temperature and RH) (Zobrist et al., 2008, 2011; Mikhailov et al., 2009; Virtanen et al., 2010; Koop et al., 2011; Tong et al., 2011; Saukko et al., 2012; Song et al., 2015; Zhang et al., 2015).

30 Variability in the phase states of atmospheric aerosols is expected to influence their hygroscopicity. For example, inhibition of mass transfer through viscous liquids or semisolid particles may result in kinetic limitations to the uptake and evaporation of water (Koop et al., 2011; Tong et al., 2011; Bones et al., 2012; Krieger et al., 2012; Pöschl and Shiraiwa, 2015). As a result, the timescales and mechanisms of condensation and evaporation may be different for liquid and solid or semisolid particles (Shiraiwa et al., 2013). Previous studies, for example, have observed extended time scales for equilibration with water vapor and/or kinetic limitations to the crystallization of ammonium sulfate for particles containing sucrose (glass transition temperature $[T_g] = 331 - 335.7$ K; Zobrist et al., 2008; Dette et al.,



2014) (Tong et al., 2011; Bones et al., 2012; Robinson et al., 2014; Hodas et al., 2015).

Variability in water vapor uptake with particle physical state also influences the activation and growth of CCN and cloud droplets (Bilde and Svenningsson, 2004; Berkemeier et al., 2014) and, thus, may impact the microphysical properties of clouds by modulating droplet number concentration. Kinetic limitations to water uptake (e.g., due to slowed rates of droplet growth) have been shown to result in as much as a 30% increase in CCN activation dry particle diameter and a decrease in cloud droplet growth rates by a factor of two (Nenes et al., 2001; Asa-Awuku et al., 2009; Raatikainen et al., 2012). Not accounting for non-ideal interactions between particle components (i.e., assuming equilibrium partitioning to an ideal solution under circumstances in which this assumption is not valid) can result in a 10 - 40% over prediction of cloud droplet number, depending on aerosol loading (Nenes et al., 2001). On the other hand, the presence of surface-active organic components can contribute to enhancements in CCN activity by reducing the surface tension of the particle surface-air interface (Ma et al., 2013; Sareen et al., 2013; Woo et al., 2013). In addition, simultaneous condensation of semivolatile organic vapors and water onto aerosol particles may enhance water uptake by increasing the availability of soluble material (Topping and McFiggans, 2012; Topping et al., 2013). This effect is expected to increase with increasing RH because the atmospheric conditions leading to higher RH (e.g., decreasing temperature) also lead to decreases in organic compound vapor pressures and, therefore, the condensation of increasingly volatile material.

Measurements of the hygroscopic growth of atmospheric aerosols in both sub- and supersaturated conditions have demonstrated discontinuities in water-uptake behavior below and above water saturation (Good et al., 2010; Irwin et al., 2010, 2011; Dusek et al., 2011; Ovadnevaite et al., 2011; Hersey et al., 2013). Specifically, for a given population of aerosols, previous studies have observed low degrees of hygroscopic growth below water saturation, but high CCN activity. Hersey et al., (2013) measured sub- and supersaturated hygroscopicity in an airborne campaign over the Los Angeles basin and observed reductions in subsaturated hygroscopic growth with increasing photochemical age of SOA and for biomass-burning aerosol, but increases in aerosol CCN activity under these same circumstances. Similarly, Good et al., (2010) found that the use of the single parameter, κ (Petters and Kreidenweis, 2007), to describe both sub- and supersaturated hygroscopic growth, as is common in models of aerosol-cloud interactions, was not sufficient to capture the water-uptake behavior of marine aerosols.

Several explanations have been put forth to reconcile observed discontinuities in water uptake below and above water saturation. A recent study suggested that for some semisolid particles (as characterized by bounce fraction), the mechanism of water uptake differs under conditions above and below water saturation, with adsorption dominating under subsaturated conditions (at RH < 95%) and absorption dominating under conditions relevant to CCN activation (Pajunoja et al., 2015). In that work, slightly oxygenated SOA derived from α -pinene and longifolene displayed water-uptake behavior under subsaturated conditions similar to that of particles comprised of SiO₂, which are known to take up water by surface adsorption. Frenkel-Halsey-Hill adsorption theory was able to describe subsaturated hygroscopic growth for these particles (Pajunoja et al., 2015). Water uptake, as modeled with the Köhler equation, is



sensitive to different parameters at low ($<95\%$) and high ($\geq 95\%$) RH, with the effects of surface tension being negligible at low RH, but important determinants of CCN activity (Wex et al., 2008). Similarly, non-ideal thermodynamic interactions are expected to be of greater importance under the more concentrated conditions relevant to subsaturated hygroscopic growth as compared to supersaturated conditions (Wex et al., 2008; Petters et al., 2009). Finally, it has been hypothesized that differences in water-uptake behavior above and below water saturation arise from variability in the prevalence of LLPS and/or the presence of solid or semisolid aerosol components with RH and temperature. High particle viscosity at subsaturated RH values can inhibit water uptake, but this effect is reduced as particle viscosity decreases with increased RH and particle liquid water content (Virtanen et al., 2010; Koop et al., 2011), possibly explaining the lower hygroscopic growth at subsaturated RH values as compared to supersaturated growth previously observed. Variability in water-uptake kinetics with RH has important implications for the activation and growth of CCN, as it suggests that the hygroscopic behavior of some particles can shift as ambient conditions transition from a subsaturated to a supersaturated regime (e.g., in an ascending air parcel).

High molecular mass compounds, such as organic oligomers, are a potential source of viscous atmospheric aerosol components. Oligomers with molecular masses ranging from 200 to 1600 g/mol have been detected in SOA generated in laboratory studies from a variety of precursors, with these compounds constituting between 25 and 70% of SOA mass (Hallquist et al., 2009 and references therein). SOA components with properties indicative of oligomers, as well as the mixture of high molecular mass compounds (likely including oligomers) termed humic-like substances (HULIS) have also been observed in the atmosphere (Kroll and Seinfeld, 2008 and references therein; Hallquist et al., 2009 and references therein; Lee et al., 2015). Barsanti and Pankow (2004, 2005, 2006) suggested that particle-phase accretion reactions could explain the presence of oligomers and esters in SOA. Laboratory studies also suggest aqueous-phase reactions lead to the formation of oligomers and esters in SOA (Altieri et al., 2008; Tan et al., 2010), with the formation of higher molecular mass compounds being favored under the more concentrated conditions relevant to aerosol liquid water as compared to the more dilute conditions of cloud droplets (Tan et al., 2010).

Because molecular mass impacts volatility, solubility, and viscosity, a more thorough understanding of the properties of aerosol components with high molar masses is needed to accurately model their behavior in large-scale atmospheric models. Utilizing laboratory surrogates for oligomers in atmospheric aerosols, we explore the influence of particle viscosity and the combined effects of LLPS and viscosity on hygroscopic growth and CCN activity and discuss the extent to which variability in viscosity is likely to be a major contributor to previously observed differences in water-uptake behavior below and above water saturation. Polyethylene glycol (PEG) was chosen as a model compound for this work because the availability of PEG with a range of polymer chain lengths/molecular masses allows for the comparison of water-uptake behavior across aerosol systems with differing viscosities, but nearly identical chemical properties. Further, previous studies of PEG-AS particles (using optical and Raman microscopy) have



shown that at $RH < \sim 90\%$, such systems undergo LLPS in which a PEG shell fully engulfs an AS core (Ciobanu et al., 2009, 2010).

2 Methods

2.1 Aerosol systems

To systematically study the influence of particle viscosity and the combined effects of LLPS and viscosity on water uptake under sub- and supersaturated RH conditions, the hygroscopic growth and CCN activity of particles comprised of PEG and mixtures of PEG and ammonium sulfate (AS) were measured with the Differential Aerosol Sizing and Hygroscopicity Spectrometer Probe (DASH-SP) and a Droplet Measurement Technologies Cloud Condensation Nuclei (DMT CCN) Counter, respectively. Experiments were conducted with aerosol systems containing PEG with average molecular masses of 200 (“PEG200”), 1,000 (“PEG1000”), and 10,000 (“PEG10000”) g mol^{-1} . This corresponds to a range in T_g from 208.15 K to 313.65 K (Pielichowski and Flejtuch, 2002; Dow, 2011). Under dry conditions and at room temperature, PEG200 is a liquid, PEG1000 is a waxy semisolid, and PEG10000 exists as solid flakes. In addition to the PEG systems, hygroscopic diameter growth factors (HGFs) and CCN activity were also measured for AS in control experiments to ensure proper instrument operation. All solutions used for aerosol generation were prepared by dissolving the reagents in Milli-Q water with resistivity $\geq 18.2 \text{ M}\Omega \text{ cm}$. For the mixed PEG-AS systems, the mass ratios of PEG:AS were 2:1 for all PEG molecular masses. The PEG oligomers were purchased from Sigma Aldrich and AS was purchased from Macron Fine Chemicals. It should be noted that the PEG are comprised of a mixture of polymers with a range of molecular masses (190 – 210 g mol^{-1} for PEG200, 950 – 1,050 g mol^{-1} for PEG1000, and 8,500 – 11,500 g mol^{-1} for PEG10000), with the number included in the name indicating the average molecular mass of the mixture. Aerosols were generated by atomizing the aqueous solutions. Before entering the DASH-SP or DMT CCN counter, atomized droplets passed through a silica gel diffusion dryer with a residence time of approximately 3 to 5 s. HGF and CCN activity measurements were conducted at room temperature ($\sim 298 \text{ K}$).

2.2 Hygroscopic growth factor measurements

HGFs were measured with the DASH-SP (Sorooshian et al., 2008) at RH values ranging from 30 to 90% in increments of 10%. After entering the DASH-SP inlet, the aerosols are further dried in a Nafion dryer (with a residence time of 1 s), they pass through a ^{210}Po neutralizer, and are then size-selected with a long-column differential mobility analyzer (DMA) based on their electrical mobility. For the HGF measurements described here, particles with dry mobility diameters of 250 nm were selected with the DMA. After size selection, the monodisperse aerosol population is split into four humidified channels, one of which is kept dry. Particle size after exposure to elevated RHs in the humidified channels is then measured at each



channel outlet with an optical particle counter (OPC). A minimum of 1500 particles is sized to generate the humidified size distributions. This was repeated 30 times within each experiment (i.e., for each aerosol system) at each RH value. OPC signal height, which is a function of both particle size and refractive index, is inverted to give particle diameter using an empirical calibration surface relating OPC signal height, refractive index, and particle size (Sorooshian et al., 2008). This surface is generated in dry calibration experiments in which OPC signal heights for salts with known refractive indices are recorded for particles with diameters ranging from 200 to 500 nm. The calculation of wet particle diameter requires knowledge of the particle's dry effective refractive index. This is measured in the dry DASH-SP channel. Wet particle diameter is determined from OPC pulse height and the calculated effective refractive index for the dry particle components by iterating on the 3-dimensional surface until agreement is achieved, within experimental uncertainty, between the wet effective refractive index as determined using this surface and a volume-weighted refractive index for the calculated wet size (taking into account the individual refractive indices for dry components and water) (Sorooshian et al., 2008). It is assumed that the particles are spherical and that they scatter, but do not absorb light. The uncertainty DASH-SP-derived droplet diameters has been shown to be ~8% at $RH < 80\%$ and ~5% at $RH \geq 80\%$ (Sorooshian et al., 2008). HGFs were calculated by dividing the wet particle diameter derived from DASH-SP measurements by the dry particle diameter (250 nm).

HGF measurements were carried out across 4 experiments with RH in the wet channels set to 30% and 40% ("experiment 1"), 50% and 60% ("experiment 2"), 70% and 80% ("experiment 3"), and 90% ("experiment 4"). For experiment 2, an overestimation in growth for the ammonium sulfate control ($HGF > 1$) led to the finding that average OPC pulse heights for the dry channel during those runs were 22% to 27% lower than average pulse heights obtained during the other experimental runs. For experiments 1, 3, and 4, on the other hand, dry-channel pulse heights for ammonium sulfate deviated by less than 5% across each experiment. The lower dry-channel pulse heights resulted in an underestimation of dry refractive index and, consequently, an overestimation of droplet growth. Similarly, dry-channel pulse heights were 12% – 14% lower on average for several of the PEG systems during experiment 2, while deviations across other experiments were typically $\leq 9\%$. Note that regardless of the humidified channel settings, it is expected that for a given aerosol system, the OPC pulse heights measured in the dry DASH-SP channel will be approximately the same across experiments. As a result, the values obtained during experiment 2 can be replaced by values obtained during other experimental runs without a substantial loss of information. Thus, for circumstances in which dry-channel pulse heights deviated by more than 10% from those measured during other experimental runs, the anomalous pulse heights were replaced by the average of the OPC pulse heights obtained during all other experimental runs; that is, the directly measured dry-channel pulse heights from experiment 2 were replaced by the value obtained by averaging pulse heights measured during experiments 1, 3, and 4. While average pulse heights are expected to produce a reasonable estimate of HGF, a higher degree of uncertainty in the HGFs existed when measured at RHs of 50% and 60%. As a result, we focus to a greater degree on the measurements conducted at the five other RH conditions.



2.3 CCN Measurements

The CCN activity of the aqueous PEG and PEG-AS aerosol systems was measured with a DMT CCN Counter (Roberts and Nenes, 2005). Similar to the DASH-SP, particles in the CCN counter are exposed to elevated RHs (in this case above water saturation, i.e., $RH > 100\%$) and then counted and sized with an OPC. Experiments were conducted at a supersaturation of 0.6%, a mid-range of the values representative of typical cloud conditions ($\sim 0.1\% - 1\%$). In the CCN counter, the supersaturation experienced by the particles is a function of both the temperature difference across the top and bottom of the instrument column and the flow rate within the column. All experiments were carried out at a total flow rate of 0.5 L min^{-1} , with a sheath flow:sample flow ratio of 10:1. Supersaturation calibrations using AS were conducted to determine the across-column temperature difference needed to achieve a supersaturation of 0.6%. For each aerosol system, CCN activity was characterized based on the critical activation diameter (D_{crit}), the diameter at which 50% of particles are activated to form CCN at a constant supersaturation (i.e., 0.6%). Prior to entering the inlet of the CCN counter, particles were size-selected with a long-column DMA and CCN counts were obtained for particles with diameters between 20 and 210 nm with a spacing of 10 nm. A condensation particle counter (CPC) sampled particles in parallel with the CCN counter to provide total particle counts, and activation fractions were calculated from the ratio of CCN concentration (C_{CCN}) to total particle concentration measured with the CPC (C_{CPC}). Measured activation fractions as a function of particle diameter were fit with a sigmoidal curve with the form $C_{CCN} / C_{CPC} = a / (1 + (x/b)^{-c})$, where a , b , and c are fit parameters and x is dry particle diameter. D_{crit} (i.e., the diameter corresponding to the sigmoid inflection point) was determined using this curve. R-square values for the sigmoidal fits ranged between 0.95 and 0.99.

2.4 Thermodynamic Modeling

To explore the extent to which observed water uptake under subsaturated RH conditions can be explained by equilibrium thermodynamic partitioning, measured HGFs were compared to calculations of hygroscopic growth at thermodynamic equilibrium. Predictions of HGF by a thermodynamic equilibrium model for the systems studied – if sufficiently accurate – allow for an interpretation of the experimental results with regard to particle viscosity. If the presence of viscosity-enhancing aerosol components (here PEG oligomers) sufficiently inhibited the uptake or evaporation of water, it is expected that measured HGFs would deviate substantially from those modeled at equilibrium. This model-measurement disagreement would occur if equilibrium growth was not achieved in the 4 s residence time of the DASH-SP humidifiers and/or if all water present in the atomized droplet could not be evaporated in the $\sim 5 \text{ s}$ total residence time in the diffusion and Nafion dryers prior to sizing in the DMA. Thus, comparison of measured HGFs with HGFs predicted at thermodynamic equilibrium provides insight into the influence of aerosol viscosity on water uptake behavior. The equilibrium model used in this study is based on the equilibrium gas-particle



partitioning framework introduced by Zuend et al. (2010) and Zuend and Seinfeld (2012). The central component of this framework is the Aerosol Inorganic-Organic Mixtures Functional groups Activity Coefficients (AIOMFAC) model (Zuend et al., 2008, 2011).

Three types of chemical equilibria are accounted for by the model in the present study: (i) vapor-liquid equilibrium (VLE) of water, (ii) a potential liquid-liquid equilibrium (LLE) affecting all components in the condensed phase, and (iii) a potential solid-liquid equilibrium of ammonium sulfate. The gas phase is treated as an ideal mixture, and water vapor is the only gas-phase component for which equilibration with the particle phase is considered. The vapor pressures of the different PEG oligomers and of AS in liquid solution are sufficiently low at 298 K that evaporation on the timescale of the experiments (total aerosol residence time ~ 10 s) is negligible. VLE of an aqueous bulk solution with a gas phase implies equivalence of the mole-fraction based water activity, a_w , with the (controlled) RH in the gas phase.

The non-ideality of liquid phases is characterized by the AIOMFAC group-contribution model (i.e., organic molecules are represented as assemblies of functional groups) in which non-ideal interactions between inorganic ions and organic functional groups in an aqueous solution are taken into account through the calculation of activity coefficients. Activity coefficients of dissolved ions and solvent compounds are quantified based on the contributions of long-range, mid-range, and short-range molecular interactions to the Gibbs excess energy of a system (Zuend et al., 2008; 2011). Included in our modeling framework is the computation of a potential LLPS, as well as the co-existence of ammonium sulfate in the crystalline state in equilibrium with the liquid organic-inorganic phases. The existence or absence of a liquid-liquid phase equilibrium is determined by solving a system of nonlinear equations to determine the phase state (i.e. a single liquid phase, or two liquid phases at LLE) that achieves a minimization of the system's overall Gibbs energy (Zuend and Seinfeld, 2013). To summarize the liquid phase treatment, AIOMFAC is applied in the equilibrium model for the computation of activity coefficients of the different mixture species in one or two co-existing liquid phases at given overall PEG/AS mass ratios and RH values.

It is well-known that the water activity and phase equilibria of PEG oligomers and polymers in aqueous solutions are rather poorly described (e.g., Ninni et al., 1999) when the standard set of functional groups is used in the UNiversal quasi-chemical Functional group Activity Coefficient model (UNIFAC; Fredenslund et al., 1975; Hansen et al., 1991) and hence also in AIOMFAC, which includes a modified UNIFAC model. In order to provide an improved model representation of aqueous PEGs (of various polymer chain lengths) and of the ternary water + PEG + AS phase diagrams, a special oxyethylene group ($-\text{CH}_2\text{-O-CH}_2-$; the repetitive monomer unit in PEG) was introduced in a recently developed PEG-specific AIOMFAC parameterization. Other system-specific AIOMFAC modifications were implemented and adjustable model parameters were determined based on published experimental data on water activities and LLE data of different water + PEG + AS systems at room temperature. A detailed description and discussion of this specific AIOMFAC parameterization will be given elsewhere (Zuend et al., *in preparation*).



Diameter HGFs, particle phase states, and phase compositions were calculated at RHs ranging from ~0 to 99% for all aerosol systems, with the exception of PEG10000-AS. For numerical and theoretical reasons, the current equilibrium model does not support a reliable calculation of LLE for high molar mass PEG oligomers. Instead, HGF calculations for the PEG10000-AS system were performed based on a
 5 Zdanovskii-Stokes-Robinson (ZSR)-like assumption, in which complete separation between phases comprised of PEG and AS is assumed at all RH values, and water uptake by the individual aerosol phases is treated separately. Total water uptake is then calculated assuming additivity of the water present in each phase. This simplification is not expected to contribute substantially to error in calculated HGFs, nor to impact model-measurement comparisons, as experimental LLE data for bulk PEG10000-AS systems
 10 suggest near-complete separation between AS and PEG up to high mole fractions of water that would be expected to occur at RH values outside the range studied in DASH-SP experiments (RH > ~95%) (Graber et al., 2007; Figure A1).

Model predictions were conducted for both hydration (low to high RH) and dehydration conditions (high to low RH). For the AS-containing systems, the hydration-case calculations account for
 15 the existence of a crystalline AS phase at SLE with the liquid phase prior to complete deliquescence of AS. In contrast, the calculations referring to the dehydration branch in the experiments were performed in a mode that allows for supersaturated conditions with respect to SLE of AS up to a critical supersaturation beyond which crystallization (efflorescence) of AS is allowed. The critical supersaturation of AS is not taken as a fixed value in terms of salt molality; rather, it is determined based on the molal ion activity
 20 product (IAP) of AS, which is defined as

$$\text{IAP}_{\text{AS}} = [a_{\text{NH}_4^+}^{(m)}]^2 [a_{\text{SO}_4^{2-}}^{(m)}]^1, \quad (1)$$

where $a_{\text{NH}_4^+}^{(m)}$ and $a_{\text{SO}_4^{2-}}^{(m)}$ are the molal activities of the ammonium and sulfate ions in solution (Zuend et al., 2010). In other words, the non-ideal interactions in the liquid solution have an effect on IAP_{AS} . This is consistent with classical nucleation theory in that the molar Gibbs energy difference (energy barrier)
 25 required for efficient nucleation of a crystalline AS phase at a certain temperature (e.g., Gao et al., 2006) is related to a critical value of IAP_{AS} . Generally, the process of nucleation-and-growth of a new crystalline phase from a liquid salt solution is stochastic in nature, yet the number of nucleation events per unit time and volume increases exponentially once a characteristic energy barrier is overcome as the supersaturation increases. In this study, the critical value of IAP_{AS} at the point of crystallization is taken (in a deterministic
 30 manner) as

$$\text{IAP}_{\text{AS}}^{(\text{crit.})} = c_{\text{AS}} \times \text{IAP}_{\text{AS}}^{(\text{sat.})}. \quad (2)$$

Here, $\text{IAP}_{\text{AS}}^{(\text{sat.})}$ is the molal ion activity product of AS at salt saturation computed by AIOMFAC for the aqueous AS system at a temperature of 298.15 K, for which the molality of AS is known from bulk measurements: $m_{\text{AS}}^{(\text{sat.})} = 5.790$ (Apelblat, 1993). The multiplication factor c_{AS} is taken as a constant
 35 coefficient relating the IAP at AS saturation to the one at crystallization in small suspended solution droplets. We determined an approximate value of $c_{\text{AS}} = 28$ by matching AIOMFAC calculations of AS



molality-dependent water activity to observed efflorescence RH obtained from electrodynamic balance (micrometer-sized aqueous AS droplets) and hygroscopicity tandem differential mobility analyzer (HTDMA; submicrometer-sized AS droplets) measurements (Zardini et al., 2008). Close to room temperature (~290 - 298 K), such experiments show that the phase transition of AS crystallization typically occurs in the range from 35% - 40% RH (Zardini et al., 2008; Ciobanu et al., 2010). With this procedure, the crystallization point (and efflorescence RH) of AS can be calculated for any mixture containing AS. In the case of the aqueous PEG-AS droplets, a liquid-liquid phase separation is predicted to be present in the RH range where AS crystallizes during a dehydration experiment. This LLPS leads to AS partitioning to a predominantly aqueous AS phase that consequently shows crystallization at approximately the same RH as in the case of the binary water + AS system.

As discussed by Hodas et al. (2015), the AIOMFAC-based model predicts phase compositions (including water), which allow for a straightforward calculation of hygroscopic mass growth factors. However, to obtain a diameter growth factor for direct comparison with the DASH-SP-determined HGFs, knowledge of the mixture density or of the partial density or volume contributions by the mixture components are necessary for the conversion. Here we assume that the particles are spherical in shape and that the partial volumes of the mixture components in the liquid phases are additive. Densities of ammonium sulfate in the solid and liquid state were obtained from Clegg and Wexler (2011). A value of $\rho_{\text{PEG200}} = 1.121 \text{ g cm}^{-3}$ is used for the liquid-state density of pure PEG200 at 298.15 K based on tabulated data by Ayranci and Sahin (2008). For pure PEG1000 and PEG10000, the (subcooled) liquid-state densities at 298.15 K were calculated based on tabulated data and density model coefficients by Mohsen-Nia et al. (2005). The values used are: $\rho_{\text{PEG1000}} = 1.1737 \text{ g cm}^{-3}$ for PEG1000 and $\rho_{\text{PEG10000}} = 1.185 \text{ g cm}^{-3}$ for PEG10000.

2.5 Estimation of water diffusivity and mixing timescale

The extent to which kinetic limitations may have contributed to the observed water uptake was further explored using the bulk diffusivity estimation scheme presented in Berkemeier et al., (2014). The bulk diffusivity of water ($D_{\text{H}_2\text{O}}$) and characteristic timescale of bulk diffusion (τ_{cd}), a metric of the time required for particles to achieve equilibrium with water vapor, were calculated at RHs ranging from 0 to 100% and at temperatures of 253 to 298 K for 250 nm particles comprised of PEG200 and PEG10000. Knowledge of τ_{cd} at 298 K provides insight into whether humidification equilibrium was likely to be reached during HGF measurements. Diffusivity estimations at temperatures < 298 K explore the influence of viscous aerosol components on water uptake at the range of temperatures experienced by particles in the troposphere, including those relevant to cloud base height.

$D_{\text{H}_2\text{O}}$ in aqueous PEG systems is parameterized based on the Vogel-Fulcher-Tamman description of the behavior of glass-forming liquids (Vogel, 1921; Fulcher, 1925; Tammann and Hesse, 1926):

$$D_{\text{H}_2\text{O}}(T, a_w) = 10^{-\left(A(a_w) + \frac{B(a_w)}{T - T_0(a_w)}\right)}, \quad (3)$$



where T is temperature, a_w is mole fraction-based water activity, A is the high-temperature maximum of $D_{\text{H}_2\text{O}}$, B is a parameter describing the functional form of diffusivity as T_g is approached, and T_0 is the temperature at which $D_{\text{H}_2\text{O}}$ approaches zero (Berkemeier et al., 2014). $A(a_w)$ and $B(a_w)$ can be estimated based on parameterizations for a chemically-similar reference compound, here sucrose (Zobrist et al., 2011), relying on the assumptions that (1) $D_{\text{H}_2\text{O}}$ of PEG and sucrose behave similarly approaching T_g (i.e., $B_{\text{sucrose}} \approx B_{\text{PEG}}$), (2) $D_{\text{H}_2\text{O}}$ is similar for PEG and sucrose at the high temperature limit (i.e., $A_{\text{sucrose}} \approx A_{\text{PEG}}$), and (3) both systems exhibit a similar ratio of T_0 to T_g (i.e., $T_{0,\text{sucrose}}/T_{0,\text{PEG}} \approx T_{g,\text{sucrose}}/T_{g,\text{PEG}}$) (Berkemeier et al., 2014). Values of a_w and T_g for PEG200 and PEG10000 were taken from the literature (Ninni et al., 1999; Pielichowski and Flejtuch, 2002; Dow et al., 2011). Calculated values of $D_{\text{H}_2\text{O}}$ were then used to estimate the e -folding time of bulk diffusion (i.e., the time required for the concentration of water in the core of a particle exposed to a given RH to be within a factor of $1/e$ of thermodynamic equilibrium) for 250 nm particles comprised of both PEG200 and PEG10000:

$$\tau_{cd} = \frac{d_p^2}{4\pi^2 D_{\text{H}_2\text{O}}}, \quad (4)$$

where d_p is particle diameter and all other parameters are as defined above (Shiraiwa et al., 2011).

3 Results and discussion

3.1 Measurements of hygroscopic growth and CCN activity

Measured HGFs for the PEG and PEG-AS systems are shown in Figure 1. For the systems containing only PEG, particles displayed moderate growth: HGFs were 1.35 for PEG200 and 1.30 for both PEG1000 and PEG10000 at an RH of 90%. In agreement with results of previous studies of the hygroscopicity of polymers and HULIS, we observed little variability in hygroscopic growth across PEG systems with different molecular masses (Brooks et al., 2004; Petters et al., 2006; Ziese et al., 2008). In general, results were similar for the PEG-AS systems; however, at RHs of 80 and 90%, greater growth was observed for PEG200-AS particles (HGFs = 1.39 and 1.60) compared to PEG1000-AS (HGFs = 1.24 and 1.38) and PEG10000-AS particles (HGFs = 1.35 and 1.42). While HGFs for the PEG10000-AS aerosols exceed those for the PEG1000-AS system at RHs of 80 and 90%, this difference is within experimental uncertainty. The large degree of similarity in HGFs for the aerosol systems containing PEG1000 and PEG10000, despite the order of magnitude difference in molecular mass, is in agreement with previous hygroscopic-growth measurements showing that the influence of polymer chain length on water uptake displays a threshold behavior, becoming relatively constant for higher degrees of polymerization (Baltensperger et al., 2005; Petters et al., 2006).

In contrast with the HGF measurements, measurements of CCN activity, as characterized by D_{crit} at a constant supersaturation of 0.6%, suggest that particle hygroscopicity at conditions of high RH increases with increasing molecular mass of the PEG polymer. CCN activity of the PEG-only containing systems was significantly diminished compared to the AS control, with D_{crit} values of 71, 66, and 60 nm for



PEG200, PEG1000, and PEG10000 respectively, compared to an activation diameter of ~ 37 nm for AS (Figures 2a, 3). The increase in CCN activity with increasing PEG molecular mass is also evident for the PEG-AS systems. Critical activation diameters were 53, 47, and 34 nm for the PEG200-AS, PEG1000-AS, and PEG10000-AS systems, respectively (Figures 2b, 3). For the systems containing only PEG, differences in D_{crit} are statistically significant for PEG200 and PEG10000 and for PEG1000 and PEG10000; however, differences in D_{crit} between PEG200 and PEG1000 are not statistically significant (Figure 3). Significant decreases in D_{crit} with increasing PEG molar mass are observed for the PEG-AS aerosol systems (Figure 3). The CCN activity of the mixed PEG10000-AS particles appears to be slightly greater than that for particles comprised only of AS, as is evident from the non-statistically significant 8% smaller D_{crit} for PEG10000-AS particles as compared to the AS control (Figure 3).

Observed increases in CCN activity with molecular mass and the enhancement in the CCN activity of PEG10000-AS compared to pure AS can likely be attributed to the fact that PEG is surface active and has been shown to lower the surface tension of the air-water interface when present in aqueous solution. The magnitude of this surface tension depression is proportional to the molecular mass of the PEG (Rey and May, 2010). Our results are also in agreement with other work suggesting that high molecular mass species (e.g., HULIS) can contribute to decreases in surface tension (Ziese et al., 2008). Sareen et al., (2013) observed that the reactive uptake of methylglyoxal and acetaldehyde resulted in enhancements in the CCN activity of AS of similar magnitude to our results for the PEG10000-AS particles (6% and 10% for methylglyoxal and acetaldehyde, respectively). In that work, the dependence of the enhancement of CCN activity on the timescales of AS exposure to organic vapors suggested that the formation of oligomers near the particle surface was a potential contributor to this effect (Sareen et al., 2013).

Our experimental results suggest a shift in the influence of molecular mass of PEG on hygroscopicity when transitioning from subsaturated RH conditions to supersaturated conditions. There are several potential factors that may have contributed to the results. First, it is possible that below water saturation, all systems experienced kinetic limitations to water uptake, preventing the particles from achieving equilibrium growth in the 4 s residence time of the DASH-SP humidifiers, potentially contributing to similarities in hygroscopic growth across the systems. As water content increases, however, particle viscosity is expected to decrease due to the plasticizing effect of water. While potentially explaining differences in hygroscopicity below and above water saturation, this does not explain why CCN activity would increase with PEG molecular mass. Second, it has been suggested that hygroscopic growth of some semisolid particles may proceed via adsorption below water saturation, but via absorption at RHs relevant to CCN activation (Pajunoja et al., 2015). Finally, the magnitude of the influence of non-ideal interactions between aerosol components, as well as other factors that influence water uptake, may differ under the concentrated conditions relevant to subsaturated hygroscopic growth as compared to water uptake in supersaturated environments. We further investigated the potential influence of these factors on experimental results by comparing measurements to predictions from the AIOMFAC model and estimations of water diffusivity and characteristic time of bulk diffusion.



3.2 Comparison of HGFs from the DASH-SP and the AIOMFAC model

Comparison between HGFs measured with the DASH-SP and those calculated with the AIOMFAC-based model at thermodynamic equilibrium provides a means to explore the potential influence of kinetic limitations to water uptake on observed hygroscopic growth. For the sake of brevity in the following discussion, the AIOMFAC-based equilibrium model predictions (described in Section 2.4) are simply referred to as “AIOMFAC predictions;” however, we note that, more precisely, the AIOMFAC model is just the core part of the equilibrium model that computes activity coefficients (and activities). Experimental results are generally in good agreement with AIOMFAC-calculated HGFs (Figures 4, 5). Because the model calculates thermodynamic equilibrium, this agreement suggests that kinetic limitations to water uptake did not strongly influence HGFs for the PEG-containing systems explored here. As noted above, if particles did not achieve equilibrium with water vapor in the ~5 s residence time of the DASH-SP dryers and/or in the 4 s residence time of the DASH-SP humidifier, it would be expected that experimental observations would deviate substantially from growth curves predicted by AIOMFAC. Model-measurement disagreement at an RH of 80% for the PEG200-AS and PEG10000-AS systems may result from uncertainty in PEG-specific AIOMFAC parameterizations and/or uncertainty in measured HGFs just above the deliquescence of AS.

The generally good agreement between AIOMFAC and HGFs measured with the DASH-SP also suggests that equilibrium absorption sufficiently describes the water-uptake behavior of the PEG aerosol systems at RHs below water saturation. Thus, it is unlikely that differences in the mechanisms of growth (i.e., adsorption versus absorption) explain the discrepancies in the influence of molecular mass on subsaturated hygroscopic growth and CCN activity observed here. This adds support to the conclusions of Pajunjoja et al. (2015) that low solubility, rather than viscosity and related kinetic limitations, drives adsorption-dominated growth at low RH for some semisolid organic aerosol constituents. While the solubility of PEG in water decreases with increasing molecular mass, PEG for all molecular masses studied here is highly water soluble (Dow et al., 2011). Thus, PEG can be considered as a surrogate for more oxygenated, aged SOA, rather than the less oxygenated SOA for which adsorptive growth was found to be important (Pajunjoja et al., 2015). While unlikely to be a major factor here, it is important to note that uncertainty in HGFs obtained with the DASH-SP, and potentially other measurement methods that derive hygroscopic growth from light scattering by particles, may be larger for systems that do experience adsorptive growth as compared to those for which water uptake is driven by absorption at all RHs. This is because calculations of HGF from DASH-SP OPC pulse heights rely on the assumption that particle refractive index can be represented as a volume-weighted average of the refractive indices of water and that of the dry particle components. This assumption may not be valid under conditions in which adsorptive growth dominates and a layer of water on the particle surface influences particle optical properties.

AIOMFAC predictions of the phase states of the aerosol systems and the prevalence of LLPS may also provide insight into other aspects of observed hygroscopic growth (Figure 5). In particular for aerosol



systems that undergo LLPS, differences in the RH at which two separated liquid phases merge to a single phase might explain the greater growth observed for the PEG200-AS system as compared to the PEG1000-AS and PEG10000-AS systems at RH of 90%. For the PEG200-AS system, AIOMFAC predicts the merging of the AS-dominated and PEG-dominated phases at an RH $\sim 86\%$, while for PEG1000-AS, LLPS is predicted to persist up to RH $\approx 94\%$ (Figure 5). With the merging of the phases for the PEG200-AS system, it is possible that more water is taken up when PEG and AS are present in a single phase than would be expected assuming that the two components take up water independently. At an RH of 90%, the model-predicted HGF for the single-phase liquid mixture comprised of PEG200 and AS is $\sim 4\%$ greater than the HGF calculated with a ZSR-type mixing rule in which water uptake by the individual aerosol components is treated separately (with total water uptake calculated in an additive manner), suggesting that this may have a small impact on observed HGFs at high RH. As noted above, complete separation between PEG10000 and AS was assumed at all RH values for the PEG10000-AS system. The validity of this assumption is supported by my modeling results for PEG200-AS and PEG1000-AS, which suggest that the RH at which separated phases merge to a single phase increases with increasing PEG molecular mass.

3.3 Water diffusivity in PEG and characteristic equilibration timescales

Calculations of $D_{\text{H}_2\text{O}}$ and τ_{cd} provide further insight into the extent to which viscosity-induced limitations to the mass transport of water in PEG may have contributed to differences in water-uptake behavior below and above water saturation. Specifically, these calculations allow us to explore whether the diffusivity of water in PEG is sufficiently slow at low and moderate RH levels that timescales for the particles to achieve equilibrium with water vapor exceed the 4 s residence time of the DASH-SP humidifier. Limitations to the mass transport of water in the particle bulk are expected to decrease with increasing RH and particle water content because water serves as a plasticizer for viscous aerosol components. As noted above, if estimations of water diffusivity and mixing timescales do suggest substantial kinetic limitations to hygroscopic growth under subsaturated conditions, this could explain, at least in part, differences in hygroscopicity below and above water saturation, but not observed increases in CCN activity with increasing PEG molecular mass.

In line with the agreement between DASH-SP and AIOMFAC HGFs, the minimal impact of kinetic limitations to water uptake on measured HGFs is supported by calculations of $D_{\text{H}_2\text{O}}$ and τ_{cd} (Figure 6). For the conditions under which experiments were conducted ($T = 298 \text{ K}$), the diffusivity of water in both PEG200 and PEG10000 is fast enough that values of τ_{cd} are predicted to be $\sim 10^{-3} \text{ s}$ at low RH. τ_{cd} decreases to $\sim 10^{-6} \text{ s}$ as RH approaches 100%. Thus, the 4 s humidification timescale in the DASH-SP is sufficient to achieve equilibrium for the PEG systems studied here. It is not expected that slow diffusion of water in PEG at subsaturated RHs contributes to the observed discrepancies in water uptake behavior above and below water saturation. This is in agreement with previous results suggesting that despite mechanical behavior indicative of solid or semisolid particles, the diffusivity of small molecules (e.g., water) in SOA



from a variety of precursors is high at room temperature (Shiraiwa et al., 2013; Price et al., 2015; Lienhard et al., 2015).

The diffusivity estimation results also provide insight into the conditions under which kinetic limitations driven by the inhibition of water transport in viscous aerosol components may be important. As is shown in Figure 6, at colder temperatures ($T = 253$ K) relevant to higher altitudes in the free troposphere, the diffusion of water in both PEG200 and PEG10000 is slowed and equilibration timescales approach 100 s, depending on ambient RH. Thus, while equilibrium partitioning sufficiently describes the water uptake behavior of PEG-containing aerosol systems under the experimental conditions considered here, this might not be the case for viscous aerosols under all atmospherically relevant conditions. It is expected that at colder ambient temperatures, increases in particle viscosity will result in larger discrepancies between water-uptake behavior below and above water saturation than observed in the present experiments. The study of water diffusivity, hygroscopic growth, and CCN activity of aerosols under a range of atmospherically relevant temperatures is an active area of research (e.g., Berkemeier et al., 2014; Price et al., 2015; Steimer et al., 2015; Lienhard et al., 2015).

3.4 Phenomena contributing to discontinuities in water-uptake behavior below and above water saturation

The supplementation of experimental results with theoretical predictions from AIOMFAC and estimations of water diffusivity suggests that observed discontinuities in the influence of PEG molecular mass on aerosol hygroscopicity under subsaturated and supersaturated RH conditions (i.e., similar growth across PEG systems at $RH < 100\%$, but increasing CCN activity with increasing molecular mass) cannot be explained by RH-dependent particle viscosity (and associated kinetic limitations to water uptake) nor differences in the mechanisms of hygroscopic growth (i.e., adsorption versus absorption). However, the ability of AIOMFAC to successfully describe the subsaturated hygroscopic growth of the PEG aerosol systems does provide insight into the factors likely to be contributing to observed differences in water-uptake behavior below and above water saturation, as AIOMFAC explicitly accounts for non-ideal interactions between aerosol components. AIOMFAC-predicted mole fraction based activity coefficients of water in PEG200, PEG1000, and PEG10000 are shown in Figure 7. It is evident that activity coefficients are substantially lower for the higher molecular mass PEGs up to an $RH \sim 95\%$, indicating a greater degree of non-ideality for those solutions. As expected, activity coefficients converge towards 1.0 (ideality) as water saturation is approached. At the RH values at which HGFs were measured, non-ideal interactions between PEG and water have a substantial influence on hygroscopic growth, while under conditions relevant to CCN activity, the influence of these non-ideal interactions is expected to be negligible (at least in the droplet bulk). Thus, we conclude that observed differences in hygroscopic growth and CCN activity can be attributed, at least in part, to the greater influence of non-ideal interactions under the more



concentrated conditions (i.e., lower water contents) relevant to subsaturated hygroscopic growth as compared to supersaturated conditions.

Our findings are in agreement with a sensitivity analysis conducted by Wex et al. (2008), in which the influence of various parameters in the Kohler model were evaluated across a range of atmospherically relevant RH values. At the more concentrated conditions relevant to hygroscopic growth below water saturation, variables influencing water activity were found to dominate in driving variability in water uptake. On the other hand, the influence of surface tension was found to be negligible at $RH < 95\%$, but to be an important determinant of growth at $RH \geq 95\%$ and particularly for CCN activity. RH-dependent variability in the degree to which surface tension influences water uptake is another likely contributor to our experimental results. Because the efficiency with which PEG depresses the surface tension of the air-particle interface is roughly proportional to the molecular mass of the PEG polymer, we observed increases in CCN activity with increasing PEG polymer chain length. However, the effects of surface tension are negligible at the RH values at which HGFs were measured with the DASH-SP, contributing to the relatively similar hygroscopic behavior across the PEG aerosol systems under subsaturated conditions. Previous work has suggested that a combination of variability in the influence of surface tension and variability in activity coefficients with degree of solute dilution contributes to differences in apparent hygroscopicity based on HGF measurements and CCN activity for HULIS particles (Wex et al., 2009; Petters et al., 2009). HULIS have been shown to have surface tensions as much as 30% lower than that of pure water at the same temperature (Kiss et al., 2005; Salma et al., 2006; Taraniuk et al., 2007).

It is important to note that in addition to RH, the influence of surface tension also varies with particle diameter. While our HGF measurements were all conducted for 250 nm particles, CCN activity was characterized based on D_{crit} at a constant supersaturation. CCN activation fractions were measured for particles with diameters ranging from 20 to 210 nm. At the smaller particle sizes, the influence of surface tension is greater, also likely contributing substantially to observed enhancements in CCN activity as compared to hygroscopic growth below water saturation. This also likely explains why our results contrast with those of Petters et al. (2006), who found evidence for decreases in CCN activity with increasing molecular mass of polymeric species. In that study, CCN activity was characterized as the critical supersaturation for particles at a set size of ~ 100 nm. Thus, the increasing efficiency of PEG as a surfactant with increasing molecular mass may not have been as evident in their measurements, as this is likely to be more important in the range of particle sizes that we studied. In addition, in that work, HGF measurements of PEG and another polymeric compound (polyacrylic acid [PAA]) were compared to CCN measurements for only PAA.

4 Atmospheric implications

Our results provide insight into the factors likely to be contributing to observed differences in ambient water-uptake behavior below and above water saturation. Specifically, they suggest that variability in the



sensitivity of hygroscopic growth to non-ideal thermodynamic interactions and surface tension depression with RH have contributed, at least in part, to these observations. Notably, in many of the circumstances in which differences in sub- and supersaturated hygroscopic behavior have been observed, oligomers and other high molecular mass compounds may have been substantial contributors to total atmospheric aerosol.

5 For example, Hersey et al. (2013) observed reductions in subsaturated hygroscopic growth but increases in CCN activity with increases in the degree of SOA aging in the eastern Los Angeles basin, where oligomeric compounds have been observed to comprise as much as 40% of submicron aerosol mass (Denkenberger et al., 2007). Differences in water-uptake behavior under sub- and supersaturated RH conditions have been observed for aerosol derived from biomass burning (Asa-Awuku et al., 2008; Dusek

10 et al., 2011; Hersey et al., 2013). HULIS have been identified as a major component of biomass burning aerosol, and laboratory studies involving levoglucosan, a tracer of biomass burning aerosol, suggest that oligomerization reactions are likely to occur in biomass burning plumes (Holmes and Petrucci, 2006, 2007). Finally, these discrepancies in aerosol water uptake below and above water saturation have been observed in marine atmospheres (Good et al., 2010; Ovadnevaite et al., 2011). It has been hypothesized that

15 the presence of biopolymers and biosurfactants in aerosol derived from sea-spray in biologically active waters contributes to this phenomena (O'Dowd et al., 2004; Ekström et al., 2010; Ovadnevaite et al., 2011).

Because the present work focuses only on compounds with a narrow range of chemical properties and experiments were conducted only at room temperature, other potential contributors to apparent differences in hygroscopicity above and below water saturation observed in ambient atmospheres (e.g.,

20 solubility limitations, slow diffusion of water in more viscous particles) cannot be ruled out. For example, estimates of the characteristic timescale for particles to achieve equilibrium with water vapor under different atmospherically relevant temperatures (Figure 6) suggest that kinetic limitations to water uptake/evaporation driven by slow diffusion in viscous aerosol components may influence discontinuities in hygroscopicity above and below water saturation to different degrees depending on ambient temperature.

25 The presence of compounds with varying solubilities that dissolve at different RHs has also been put forth as a potential explanation for enhanced CCN activity as compared to subsaturated hygroscopic growth (Petters et al., 2009). While it is possible that due to the range of molecular masses present in each PEG reagent, lower molecular mass components dissolve into solution at lower RH values while higher molecular mass components did not dissolve until RH approached 100%, given the overall high solubility

30 of PEG, it is unlikely that this had any substantial impact on our results. However, this phenomenon may be more important for ambient aerosol, in which compounds with a wider range of water solubilities are present.

The results of the present work also have implications for hygroscopicity measurements and the representation of aerosol hygroscopicity in large-scale atmospheric models. First, they suggest that the use

35 of a single hygroscopicity parameter (e.g., κ) derived from HGF measurements may lead to a substantial underestimation of CCN activity in environments in which oligomers, other high molecular mass compounds, and surface-active components are present in atmospheric aerosols. In addition, due to the



greater influence of surface tension depression on water uptake for smaller particles, the way in which CCN activity is quantified may result in substantial differences in hygroscopicity characterization. For example, calculation of D_{crit} from CCN activation fraction measurements conducted at a single supersaturation may result in a greater apparent hygroscopicity than if determined based on calculations of critical supersaturation, in which activation fractions of particles of a constant, typically larger diameter are measured for a range of supersaturations.

5 Conclusions

We observed a shift in the influence of molecular mass on the water-uptake behavior of surrogates for oligomers in atmospheric aerosol when transitioning from subsaturated to supersaturated RH conditions. A comparison of experimental and modeling investigations of water-uptake behavior of PEGs with a range of molecular masses and viscosities suggests that apparent discrepancies in hygroscopicity above and below water saturation can be attributed, at least in part, to a combination of RH-dependent differences in the sensitivity of water uptake behavior to non-ideal interactions and to surface tension effects. Under the experimental conditions investigated here, there was no evidence that kinetic limitations to water uptake due to the presence of viscous aerosol components inhibited water uptake at lower RH, nor that hygroscopic growth was driven by adsorption at low RH and absorption at high RH. This finding supports the hypothesis that limitations in solubility, rather than particle viscosity, drive the dominance of adsorptive growth at low RH observed for some semisolid particles. The accurate description of subsaturated hygroscopic growth of particles comprised of AS and the oxidized oligomers for which PEG serves as a surrogate requires the consideration of non-ideal thermodynamic interactions between these aerosol components, including the potential presence of LLPS, as is achieved by thermodynamic models like the one based on AIOMFAC.

Acknowledgements. This work was supported by the Office for Naval Research under award no. N00014-14-1-0097. Natasha Hodas was supported by a National Science Foundation Atmospheric and Geospace Sciences Postdoctoral Research Fellowship, award no. 14433246. The authors gratefully acknowledge helpful discussions with Armin Sorooshian and Taylor Shingler regarding the DASH-SP.



References

- Altieri, K. E., Seitzinger, S. P., Carlton, A. G., Tuprin, B. J., Klein, G. C., and Marshall, A. G.: Oligomers formed through in-cloud methylglyoxal reactions: chemical composition, properties, and mechanisms investigated by ultra-high resolution FT-ICR mass spectrometry, *Atmos. Environ.*, 42, 1476-1490, 2008.
- Apelblat, A.: The vapour pressures of saturated aqueous solutions of potassium bromide, ammonium sulfate, copper(II) sulfate, iron(II) sulfate, and manganese(II) dichloride, at temperatures from 283 K to 308 K, *J. Chem. Thermodyn.*, 25, 1513-1520, 1993.
- Ayranci, E., and Sahin, M.: Interactions of polyethylene glycols with water studied by measurements of density and sound velocity, *J. Chem. Thermodyn.*, 40, 1200-1207, 2008.
- Asa-Awuku, A., Sullivan, A. P., Hennigan, C. J., Weber, R. J., and Nenes, A.: Investigation of molar volume and surfactant characteristics of water-soluble organic compounds in biomass burning aerosol, *Atmos. Chem. Phys.*, 8, 799-812, 2008.
- Asa-Awuku, A., Engelhart, G. J., Lee, B. H., Pandis, S. N., and Nenes, A.: Relating CCN activity, volatility, and droplet growth kinetics of β -caryophyllene secondary organic aerosol, *Atmos Chem Phys*, 9, 795- 812, 2009.
- Baltensperger, U., Kalberer, M., Dommen, J., Paulsen, D., Alfarra, M. R., Coe, H., Fisseha, R., Gascho, A., Gysel, M., Nyeki, S., Sax, M., Steinbacher, M., Prevot, A. S. H., Sjögren, S., Weingartner, E., and Zenobi, R.: Secondary organic aerosols from anthropogenic and biogenic precursors, *Farraday Discuss.*, 130, 265-278, 2005.
- Barsanti, K. C. and Pankow, J. F.: Thermodynamics of the formation of atmospheric organic particulate matter by accretion reactions-Part 1: Aldehydes and ketones, *Atmos. Environ.*, 38, 4371-4382, 2004.
- Barsanti, K. C. and Pankow, J. F.: Thermodynamics of the formation of atmospheric organic particulate matter by accretion reactions-2: Dialdehydes, methylglyoxal, and diketones, *Atmos. Environ.*, 39, 6597-6607, 2005.
- Barsanti, K. C. and Pankow, J. F.: Thermodynamics of the formation of atmospheric organic particulate matter by accretion reactions-Part 3: Carboxylic and dicarboxylic acids, *Atmos. Environ.*, 40, 6676-6686, 2006.
- Berkemeier, T., Shiraiwa, M., Pöschl, U., and Koop, T.: Competition between water uptake and ice nucleation by glass organic aerosol particles, *Atmos. Chem. Phys*, 15, 12513-12531, 2014.
- Bertram, A. K., Martin, S. T., Hanna, S. J., Smith, M. L., Bodsworth, A., Chen, Q., Kuwata, M., Liu, A., You, Y., and Zorn, S. R.: Predicting the relative humidities of liquid-liquid phase separation, efflorescence, and deliquescence of mixed particles of ammonium sulfate, organic material, and water using the organic-to-sulfate mass ratio of the particle and the oxygen-to-carbon elemental ratio of the organic component, *Atmos. Chem. Phys.*, 11, 10995–1006, 2011.



- Bilde, M. and Svenningsson, B.: CCN activation of slightly soluble organics: the importance of small amounts of inorganic salts and particle phase. *Tellus B*, 56, 128-134, 2004.
- Bones, D. L., Reid, J. P., Lienhard, D. M., and Krieger, U. K.: Comparing the mechanism of water condensation and evaporation in glassy aerosol, *Proc. Natl. Acad. Sci.*, 109, 11613 – 11618, 2012.
- 5 Boucher, O., Randall, D., Artaxo, P., Bretherton, C., Feingold, G., Forster, P., Kerminen, V.-M., Kondo, Y., Liao, H., Lohman, U., Rasch, P., Satheesh, S. K., Sherwood, S., Stevens, B., and Zhang, X. Y.: Clouds and Aerosols, in: *Climate Change 2013: The Physical Science Basis. Contribution of Working Group I to the Fifth Assessment Report of the Intergovernmental Panel on Climate Change* [Stocker, T. F., Qin, D., Plattner, G.-K., Tignor, M., Allen, S.K., Boschung, J., Nauels, A., Xia, Y., Bex, V., and Midgley, P. M. (eds.)]. Cambridge University Press, Cambridge, United Kingdom and New York, NY, USA, 2013.
- 10 Brooks, S. D., DeMott, P. J., and Kreidenweis, S. M.: Water uptake by particles containing humic materials with ammonium sulfate, *Atmos. Environ.*, 38, 1859-1868, 2004.
- 15 Ciobanu, V. G., Marcolli, C., Krieger, U. K., Weers, U., and Peter, T.: Liquid-liquid phase separation in mixed organic/inorganic aerosol particles. *J. Phys. Chem.*, 113 10966–10978, 2009.
- Ciobanu, V. G., Marcolli, C., Krieger, U. K., Zuend, A., and Peter, T.: Efflorescence of ammonium sulfate and coated ammonium sulfate particles: Evidence for surface nucleation, *J. Phys. Chem. A*, 114, 9486-9495, 2010.
- 20 Clegg, S. L. and Wexler, A. S.: Densities and Apparent Molar Volumes of Atmospherically Important Electrolyte Solutions. 1. The Solutes H_2SO_4 , HNO_3 , HCl , Na_2SO_4 , NaNO_3 , NaCl , $(\text{NH}_4)_2\text{SO}_4$, NH_4NO_3 , and NH_4Cl from 0 to 50 °C, including extrapolations to very low temperature and to the pure liquid state, and NaHSO_4 , NaOH , and NH_3 at 25 °C, *J. Phys. Chem. A*, 115, 3393-3460, 2011.
- 25 Dette, H. P., Qi, M., Scroder, D. C., Godt, A., and Koop, T.: Glass-forming properties of 3-methylbutane-1,2,3-tricarboxylic acid and its mixtures with water and pinonic acid, *J. Phys. Chem. A*, 118, 7024-7033, 2014.
- Denkenberger, K. A., Moffet, R. C., Holecek, J. C., Rebotier, T. P., and Prather, K. A.: Real-time, single-particle measurements of oligomers in aged ambient aerosol particles, *Environ. Sci. Technol.*, 41, 5439-5446, 2007.
- 30 Dow Chemical Company: Carbowax polyethylene glycols, Form No 118-01789-1011 AMS, 2011.
- Dusek, U., Frank, G. P., Massling, A., Zeromskiene, K., Iinuma, Y., Schmid, O., Helas, G., Hennig, T., Wiedensohler, A., and Andreae, M. O.: Water uptake by biomass burning aerosol at sub- and supersaturated conditions: Closure studies and implications for the role of organics. *Atmos. Chem. Phys.*, 11, 9519-9523, 2011.
- 35



- Ekström, S. Nozière, B., Hultberg, M., Alsberg, T., Magnér, J., Nilsson, E. D., and Artaxo, P.: A possible role of ground-based microorganisms on cloud formation in the atmosphere, *Biogeosciences*, 7, 387-394, 2010.
- 5 Erdakos, G. B. and Pankow, J. F.: Gas/particle partitioning of neutral and ionizing compounds to single- and multi-phase aerosol particles. 2. Phase separation in liquid particulate matter containing both polar and low-polarity organic compounds, *Atmos. Environ.*, 38, 1005 – 1013, 2004.
- Fredenslund, A., Jones, R. L., and Prausnitz, J. M.: Group-Contribution Estimation of Activity Coefficients in Nonideal Liquid Mixtures, *AIChE J.*, 21, 1086–1099, 1975.
- 10 Fulcher, G. S.: Analysis of recent measurements of the viscosity of glasses, *J. Am. Ceram. Soc.*, 8, 339-355, 1925.
- Gao, Y. G., Chen, S. B., Yu, L. E.: Efflorescence Relative Humidity for Ammonium Sulfate Particles. *J. Phys. Chem. A*, 110, 7602-7608, 2006.
- Good, N., Topping, D. O., Allan, J. D., Flynn, M., Fuentes, E., Irwin, M., Williams, P. I., Coe, H., and McFiggans, G.: Consistency between parametrisations of aerosol hygroscopicity and CCN
- 15 activity during the RHaMBLe discovery cruise, *Atmos. Chem. Phys.*, 10, 3189-3203, 2010.
- Graber, T. A., Medina, H., Galleguillos, H. R., and Taboada, M. E.: Phase equilibrium and partition of iodide in a aqueous biphasic system formed by $(\text{NH}_4)_2\text{SO}_4 + \text{PEG} + \text{H}_2\text{O}$ at 25°C, *J. Chem. Eng. Data*, 52, 1262-1267, 2007.
- Hallquist M., Wenger J. C., Baltensperger U., Rudich Y., Simpson D., Claeys M., Dommen J., Donahue N.
- 20 M., George C., Goldstein A. H., Hamilton J. F., Herrmann H., Hoffmann T., Iinuma Y., Jang M., Jenkin M. E., Jimenez J. L., Kiendler-Scharr A., Maenhaut W., McFiggans G., Mentel, T. F., Monod A., Prevot A. S. H., Seinfeld J. H., Surratt J. D., Szmigielski R., and Wildt J.: The formation, properties and impact of secondary organic aerosol: current and emerging issues, *Atmos. Chem. Phys.*, 9, 5155-5236, 2009.
- 25 Hansen, H. K., Rasmussen, P., Fredenslund, A., Schiller, M., and Gmehling, J.: Vapor-liquid-equilibria by UNIFAC group contribution. 5. Revision and extension, *Ind. Eng. Chem. Res.*, 30, 2352–2355, 1991.
- Hersey, S. P., Craven, J. S., Metcalf, A. R., Lin, J., Lathem, T., Suski, K. J., Cahill, J. F., Duong, H. T., Sorooshian, A., Jonsson, H. H., Shiraiwa, M., Zuend, A., Nenes, A., Prather, K. A., Flagan, R.
- 30 C., and Seinfeld, J. H.: Composition and hygroscopicity of the Los Angeles aerosol: CalNex. *J. Geophys. Res.*, 118, 3016-3036, 2013.
- Hodas, N., Zuend, A., Mui, W., Flagan, R. C., and Seinfeld, J. H.: Influence of particle-phase state on the hygroscopic behavior of mixed organic-inorganic aerosols, *Atmos. Chem. Phys.*, 15, 5027-5045, 2015.
- 35 Holmes, B. J. and Petrucci, G. A.: Water-soluble oligomer formation from acid-catalyzed reactions of levoglucosan in proxies of atmospheric aqueous aerosols, *Environ. Sci. Technol.*, 40, 4983-4989, 2006.



- Holmes, B. J. and Petrucci, G. A.: Oligomerization of levoglucosan by Fenton chemistry in proxies of biomass burning aerosols, *J. Atmos. Chem.*, 58, 151-166, 2007.
- Irwin, M., Good, N., Crosier, J., Choularton, T. W., and McFiggans, G.: Reconciliation of measurements of hygroscopic growth and critical supersaturation of aerosol particles in central Germany, *Atmos. Chem. Phys.*, 10, 11737-11752, 2010.
- Irwin, M., Robinson, N., Allan, J.D., Coe, H., and McFiggans, G.: Size-resolved water uptake and cloud condensation nuclei measurements as measured above a Southeastern Asian rainforest during OP3, *Atmos. Chem. Phys.*, 11, 11157-11174, 2011.
- Kiss, G., Tombacz, E., and Hansson, H.-C.: Surface tension effects of humic-like substances in the aqueous extract of tropospheric fine aerosol, *J. Atmos. Chem.*, 50, 279-294, 2005.
- Koop, T., Bookhold, J., Shiraiwa, M., and Pöschl, U.: Glass transition and phase state of organic compounds: dependency on molecular properties and implications for secondary organic aerosols in the atmosphere, *Phys. Chem. Chem. Phys.*, 13, 1923-19255, 2011.
- Krieger, U., Marcolli, C., and Reid, J. P.: Exploring the complexity of aerosol particle properties and processes using single particle techniques, *Chem. Soc. Rev.*, 41, 6631-6662, 2012.
- Kroll, J. H. and Seinfeld, J. H.: Secondary organic aerosol: Formation and evolution of low-volatility organics in the atmosphere, *Atmos Environ.*, 42, 3593-3624, 2008.
- Lee, A. K. Y., Willis, M. D., Heay, R. M., Wang, J. M., Jeong, C.-H., Wenger, J. C., Evans, G. J., and Abbatt, J. P. D.: Single particle characterization of biomass burning organic aerosol (BBOA): Evidence for non-uniform mixing of high molecular mass organics and potassium, *Atmos. Chem. Phys. Discuss.*, 15, 32157-32183, 2015.
- Lienhard, D. M., Huisman, A. J., Krieger, U. K., Rudich, Y., Marcolli, C., Luo, B. P., Bones, D. L., Reid, J. P., Lambe, A. T., Canagaratna, M. R., Davidovits, P., Onasch, T. B., Worsnop, D. R., Steimer, S. S., Koop, T., and Peter, T.: Viscous organic aerosol particles in the upper troposphere: Diffusivity-controlled water uptake and ice nucleation?, *Atmos. Chem. Phys.*, 15, 13599-13613, 2015.
- Ma, Y., Brooks, S. D., Vidaurre, G., Khalizov, A. F., Wang, L., and Zhang, R.: Rapid modification of cloud-nucleating abilities of aerosols by biogenic emissions, *Geophys. Res. Lett.*, 40, 6293-6297, 2013.
- McNeill, V. F.: Aqueous organic chemistry in the atmosphere: Sources and chemical processing of organic aerosols, *Environ. Sci. Technol.*, 49, 1237-1244, 2015.
- Mikhailov, E., Vlasenko, S., Martin, S. T., Koop, T., and Pöschl, U.: Amorphous and crystalline aerosol particles interacting with water vapor: conceptual framework and experimental evidence for restructuring, phase transitions and kinetic limitations, *Atmos. Chem. Phys.*, 9, 9491-9522, 2009.



- Mohsen-Nia, M., Modarress, H., and Rasa, H.: Measurement and Modeling of Density, Kinematic Viscosity, and Refractive Index for Poly(ethylene Glycol) Aqueous Solution at Different Temperatures, *J. Chem. Eng. Data*, 50, 1662-1666, 2005.
- 5 Nenes, A., Chan S., Abdul-Razzak, H., Chuan, P. Y., and Seinfeld, J. H.: Kinetic limitations on cloud droplet formation and impact on cloud albedo. *Tellus B*, 53, 133-149, 2001.
- Ninni, L. Camargo, M. S., and Meirelles, A. J. A.: Water activity in poly(ethylene glycol) aqueous solutions, *Thermochim. Acta*, 328, 169-176, 1999.
- O'Dowd, C. O. Facchini, M. C., Cavalli, F., Cebumis, D., Mircea, M., Decesari, S., Fuzzi, S., Yoon, Y. J., and Putaud, J.-P.: Biogenically driven organic contribution to marine aerosol, *Nature*, 431, 676-10 680, 2004.
- Pajunoja, A., Lambe, A. T., Hakala, J., Rastak, N., Cummings, M. J., Brogan, J. F., Hao, L., Paramonov, M., Hong, J., Prisle, N. L., Malila, J., Romakkaniemi, S., Lehtinen, K. E., Laaksonen, A., Kulmala, M., Massoli, P., Onasch, T. B., Donahue, N. M., Riipinen, I., Davidovits, P., Worsnop, D. R., Petäjä, T., and Virtanen, A.: Adsorptive uptake of water by semisolid 15 secondary organic aerosol, *Geophys. Res. Lett.*, 42, 3063-3068, 2015.
- Petters, M. D., Kreidenweis, S. M., Snider, J. R., Koehler, K. A., Wang, Q., Prenni, A. J., and Demott, P. J.: Cloud droplet activation of polymerized organic aerosol, *Tellus B*, 58, 196-205, 2006.
- Petters, M. D. and Kreidenweis, S. M.: A single parameter representation of hygroscopic growth and cloud condensation nucleus activity, *Atmos. Chem. Phys*, 7, 1961-1971, 2007.
- 20 Petters, M. D., Wex, H., Carrico, C. M., Hallbauer, E., Massling, A., McMeeking, G. R., Poulain, L., Wu, Z., Sreidenweis, S. M., and Stratmann, F.: Towards closing the gap between hygroscopic growth and activation for secondary organic aerosol- Part 2: Theoretical approaches, *Atmos. Chem. Phys*, 9, 3999-4009, 2009.
- Pielichowski, K. and Flejtuch, K.: Differential scanning calorimetry studies on poly(ethylene) glycol with 25 different molecular masses for thermal energy storage materials, *Polym. Adv. Technol.*, 13, 690-696, 2002.
- Pöhlker, C., Wiedemann, K. T., Sinha, B., Shiraiwa, M., Gunthe, S. S., Smith, M., Su, H., Artaxo, P., Chen, Q., Cheng, Y. F., Elbert, W., Gilles, M. K., Kilcoyne, A. L. D., Moffet, R. C., Weigand, M., Martin, S. T., Pöschl, U., and Andreae, M. O.: Biogenic potassium salt particles as seeds for 30 secondary organic aerosol in the Amazon, *Science* 337, 1075-1078, 2012.
- Pöschl, U. and Shiraiwa, M.: Multiphase chemistry at the atmosphere-biosphere interface influencing climate and public health in the Anthropocene, *Chem. Rev.*, 115, 4440-4475, 2015.
- Price, H. C., Mattsson, J., Zhang, Y., Bertram, A. K., Davies, J. F., Grayson, J. W., Martin, S. C., O'Sullivan, D., Reid, J. P., Rickards, A. M. J., and Murray, B. J.: Water diffusion in 35 atmospherically-relevant α -pinene secondary organic matter, *Chem. Sci.*, 6, 4876-4883, 2015.



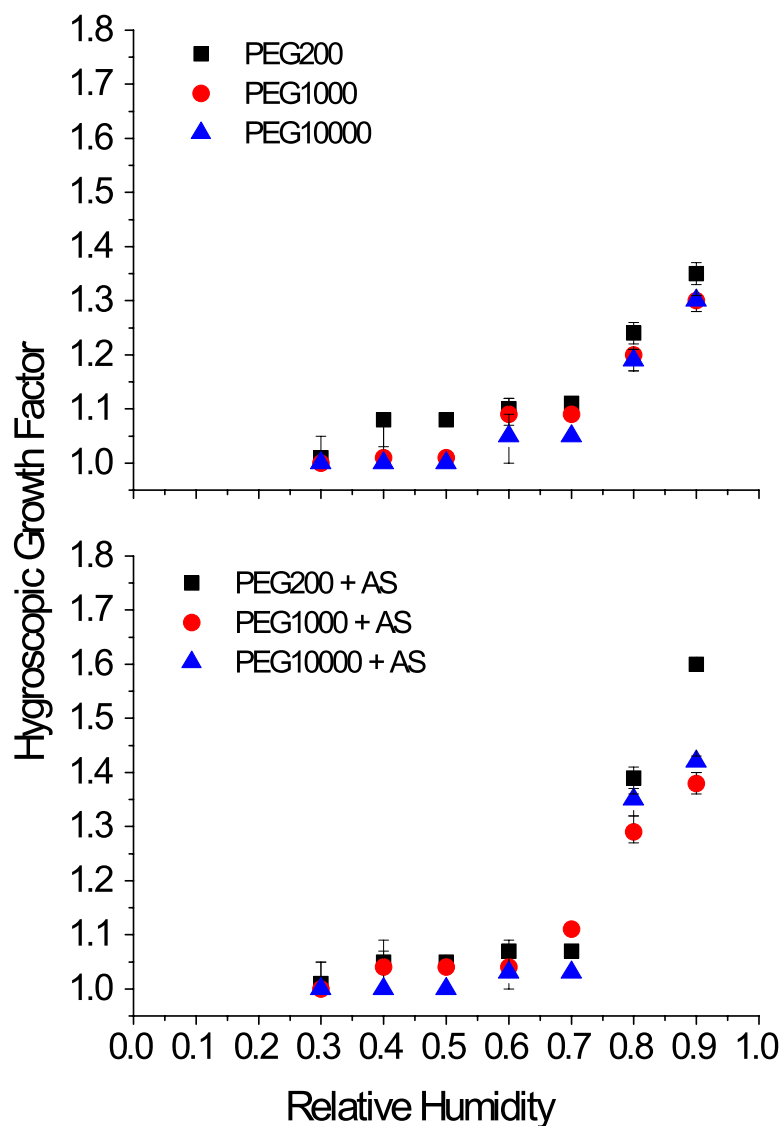
- Raatikainen, T., Moore, R. H., Lathem, T. L., and Nenes, A.: A coupled observation-modeling approach for studying activation kinetics from measurements of CCN activity, *Atmos. Chem. Phys.*, 12, 4227-4243, 2012.
- Rey, L. and May, J. C.: Freeze drying/lyophilization of pharmaceutical and biological particles, 3rd edition, Informa Healthcare, New York, NY, 2010.
- Roberts, G. C. and Nenes, A.: A continuous-flow streamwise thermal-gradient CCN chamber for atmospheric measurements, *Aerosol Sci. Technol.*, 39, 206-221, 2005.
- Robinson, C. B., Schill, G. P., and Tolbert, M. A.: Optical growth of highly viscous organic/sulfate particles, *J. Atmos. Chem.*, 71, 145-156, 2014.
- 10 Sareen, N., Schwier, A. N., Lathem, T. L., Nenes, A., and McNeill, V. F.: Surfactants from the gas phase may promote cloud droplet formation, *Proc. Natl. Acad. Sci.*, 110, 2723-2728.
- Salma, I., Ocskay, R., Varga, I., and Maenhaut, W.: Surface tension of atmospheric humic-like substances in connection with relaxation, dilution, and solution ph, *J. Geophys. Res.*, 111, D23205, doi:10.1029/2005JD007015, 2006.
- 15 Saukko, E., Lambe A. T., Massoli, P., Koop, T., Wright, J. P., Croasdale, D. R., Pederna, D. A., Onasch, T. B., Laaksonen, A., Davidovits, P., Worsnop, D. R., and Virtanen, A.: Humidity-dependent phase state of SOA particles from biogenic and anthropogenic precursors, *Atmos. Chem. Phys.*, 12, 7515–7529, 2012.
- Seinfeld, J. H. and Pandis, S. N.: Atmospheric chemistry and physics: From air pollution to climate change, 2nd edition, Jon Wiley & Sons, Inc., Hoboken, NJ, 2006.
- 20 Shiraiwa, M., Ammann, M., Koop, T., and Poschl, U. Gas uptake and chemical aging of semisolid organic aerosol particles, *PNAS*, 108, 11003-11008, 2011.
- Shiraiwa M., Zuend, A., Bertram, A. K., and Seinfeld, J. H.: Gas-particle partitioning of atmospheric aerosols: interplay of physical state, non-ideal mixing and morphology, *Phys. Chem. Chem. Phys.*, 15, 11441-11453, 2013.
- 25 Song, M., Marcolli, C., Krieger, U. K., Zuend, A., and Peter, T.: Liquid-liquid phase separation and morphology of internally mixed dicarboxylic acids/ammonium sulfate/water particles, *Atmos. Chem. Phys.*, 12, 2691-2712, 2012.
- Song, M., Liu, P. F., Hanna, S. J., Martin, S. T., and Bertram, A. K.: Relative-humidity dependent viscosities of isoprene-derived secondary organic material and atmospheric implications for isoprene-dominant forests, *Atmos. Chem. Phys. Discuss.*, 15, 1131-1169, 2015.
- 30 Sorooshian A., Hersey C., Brechtel F. J., Corless A., Flagan R. C., and Seinfeld J. H.: Rapid, size-resolved aerosol hygroscopic growth measurements: Differential Aerosol Sizing and Hygroscopicity Spectrometer Probe (DASH-SP). *Aerosol Sci. Technol.*, 42,445-464, 2008.
- 35 Steimer, S. S., Krieger, U. K., Te, Y.-F., Lienhard, D. M., Huisman, A. J., Ammann, M., and Peter, T.: Electrodynamical balance measurements of thermodynamic, kinetic, and optical aerosol properties inaccessible to bulk methods, *Atmos. Meas. Tech. Discuss.*, 8, 689-719, 2015.



- Tammann, G., and Hesse, W.: The dependency of viscosity on temperature in hypothermic liquids, *Z. Anorg. Allg. Chem.*, 156, 14, 1926.
- Tan, Y., Carlton, A. G., Seitzinger, S. P., and Turpin, B. J.: SOA from methylglyoxal in clouds and wet aerosols: Measurement and prediction of key products, *Atmos. Environ.* 44, 5218-5226, 2010.
- 5 Taraniuk, I., Graber, E. R., Kostinski, A., and Rudich, Y.: Surfactant properties of atmospheric and model humic-like substances (HULIS), *Geophys. Res. Lett.*, 34, L16807, doi:10.1029/2007GL029576, 2007.
- Tong, H.-J., Reid, J. P., Bones, D. L., Luo, B. P., and Krieger, U. K.: Measurements of the timescales for the mass transfer of water in glassy aerosol at low relative humidity and ambient temperature, *Atmos. Chem. Phys.*, 11, 4739-4754, 2011.
- 10 Topping, D. O. and McFiggans, G.: Tight coupling of particle size, number and composition in atmospheric cloud droplet activation, *Atmos. Chem. Phys.*, 12, 3253-3260, 2012.
- Topping, D., Connolly, P., and McFiggans, G.: Cloud droplet number enhanced by co-condensation of organic vapours, *Nature Geoscience*, 6, 443-446, 2013.
- 15 Virtanen, A., Joutsensaari, J., Koop, T., Kannosto, J., Yli-Pirila, P., Leskinen, J., Makela, J. M., Holopainen, J. K., Poschl, U., Kulmala, M., Worsnop, D. R., and Laaksonen A. An amorphous solid state of biogenic secondary organic particles. *Nature*, 467, 824-827, 2010.
- Vogel, H.: The temperature dependence law of the viscosity of fluids, *Physik. Z.*, 22, 645-198 646, 1921.
- Wex, H., Stratmann, F., Topping, D., and McFiggans, G.: The Kelvin versus the Raoult term in the Kohler equation, *J. Atmos. Sci.*, 65, 4004-4016, 2008.
- 20 Wex, H., Petters, M. D., Carrico, C. M., Hallbauer, E., Massling, A., McMeeking, G. R., Poulain, L., Wu, Z., Kreidenweis, S. M., and Stratmann, F.: Towards closing the gap between hygroscopic growth and activation for secondary organic aerosol: Part 1 – Evidence from measurements, *Atmos. Chem. Phys.*, 9, 3987-3997, 2009.
- 25 Woo, J. L., Kim, D. D., Schweier, A. N., Li, R., and McNeill, V. F.: Aqueous aerosol SOA formatin: impact on aerosol physical properties, *Faraday Disciss.*, 165, 357-367, 2013.
- You, Y., Renbaum-Wolff, L., Carreras-Sospedra, M., Hanna, S. J., Hiranuma, N., Kamal, S., Smith, M. L., Zhang, X. L., Weber, R. J., Shilling, J. E., Dabdub, D., Martin, S. T., and Bertram, A. K.: Images reveal that atmospheric particles can undergo liquid-liquid phase separations, *Proc. Natl. Acad. Sci.*, 109, 13188-13193, 2012.
- 30 You, Y., Renbaum-Wolff, L., and Bertram, A. K.: Liquid-liquid phase separation in particles containing organics mixed with ammonium sulfate, ammonium bisulfate, ammonium nitrate, or sodium chloride, *Atmos. Chem. Phys.*, 13, 11723-11734, 2013.
- 35 You, Y., Smith, M. L., Song, M., Martin, S. T., and Bertram, A. K.: Liquid-liquid phase separation in atmospherically relevant particles consisting of organic species and inorganic salts, *Int. Rev. Phys. Chem.*, 33, 43-77, 2014.



- Zardini, A. A., Sjogren, S., Marcolli, C., Krieger, U. K., Gysel, M., Weingartner, E., Baltensperger, U., and Peter, T.: A combined particle trap/HTDMA hygroscopicity study of mixed inorganic/organic aerosol particles, *Atmos. Chem. Phys.*, 8, 5589–5601, 2008.
- 5 Zhang, Y., Sanchez, M. S., Douet, C., Wang, Y., Bateman, A. P., Gong, Z., Kuwata, M., Renbaum-Wolff, L., Sato, B. B., Liu, P. F., Bertram, A. K., Geiger, F. M., and Martin, S. T.: Changing shapes and implied viscosities of suspended submicron particles, *Atmos. Chem. Phys. Discuss.*, 15, 6821–6850, 2015.
- 10 Ziese, M. Wex, H., Nilsson, E., Ocskay, R., Henning, T., Massling, A., and Stratmann, F.: Hygroscopic growth and activation of HULIS particles: Experimental data and a new iterative parameterization scheme for complex aerosol particles, *Atmos. Chem. Phys.*, 8, 1855–1866, 2008.
- Zobrist, B., Marcolli, C., Pedernera, D. A., and Koop, T. Do atmospheric aerosols form glasses? *Atmos. Chem. Phys.*, 8, 5221–5244, 2008.
- 15 Zobrist, B., Soonsin, V., Luo, B. P., Krieger, U. K., Marcolli, C., Peter, T., Koop, T.: Ultra-slow water diffusion in aqueous sucrose glasses, *Phys. Chem. Chem. Phys.*, 13, 3514–3526, 2011.
- Zuend, A., Marcolli, C., Luo, B. P., and Peter T.: A thermodynamic model of mixed organic-inorganic aerosols to predict activity coefficients, *Atmos. Chem. Phys.*, 8, 4559–4593, 2008.
- 20 Zuend, A., Marcolli, C., Peter, T., and Seinfeld, J. H.: Computation of liquid-liquid equilibria and phase stabilities: implications for RH-dependent gas/particle partitioning of organic-inorganic aerosols, *Atmos. Chem. Phys.*, 10, 7795–7820, 2010.
- Zuend, A., Marcolli, C., Booth, A. M., Lienhard, D. M., Soonsin, V., Krieger, U. K., Topping, D. O., McFiggans, G., Peter, T., and Seinfeld J. H.: New and extended parameterization of the thermodynamic model AIOMFAC: calculation of activity coefficients for organic-inorganic mixtures containing carboxyl, hydroxyl, carbonyl, ether, ester, alkenyl, alkyl, and aromatic functional groups, *Atmos. Chem. Phys.*, 11, 9155–9206, 2011.
- 25 Zuend, A. and Seinfeld, J. H.: Modeling the gas-particle partitioning of secondary organic aerosol: the importance of liquid-liquid phase separation. *Atmos. Chem. Phys.*, 12, 3857–3882, 2012.
- 30 Zuend, A. and Seinfeld, J. H.: A practical method for the calculation of liquid-liquid equilibria in multicomponent organic-water-electrolyte systems using physiochemical constraints, *Fluid Phase Equilibria*, 337, 201–213, 2013.



5 **Figure 1.** Measured hygroscopic growth factors (HGFs) for aerosol systems comprised only of PEG (top)
 and aerosol systems comprised of PEG and ammonium sulfate (AS) with PEG:AS mass ratios of 2:1
 (bottom). HGFs were measured for particles with diameters of 250 nm. Symbols indicate the average HGF,
 and error bars indicate the maximum and minimum HGFs derived from repeated measurements with the
 DASH-SP.

10

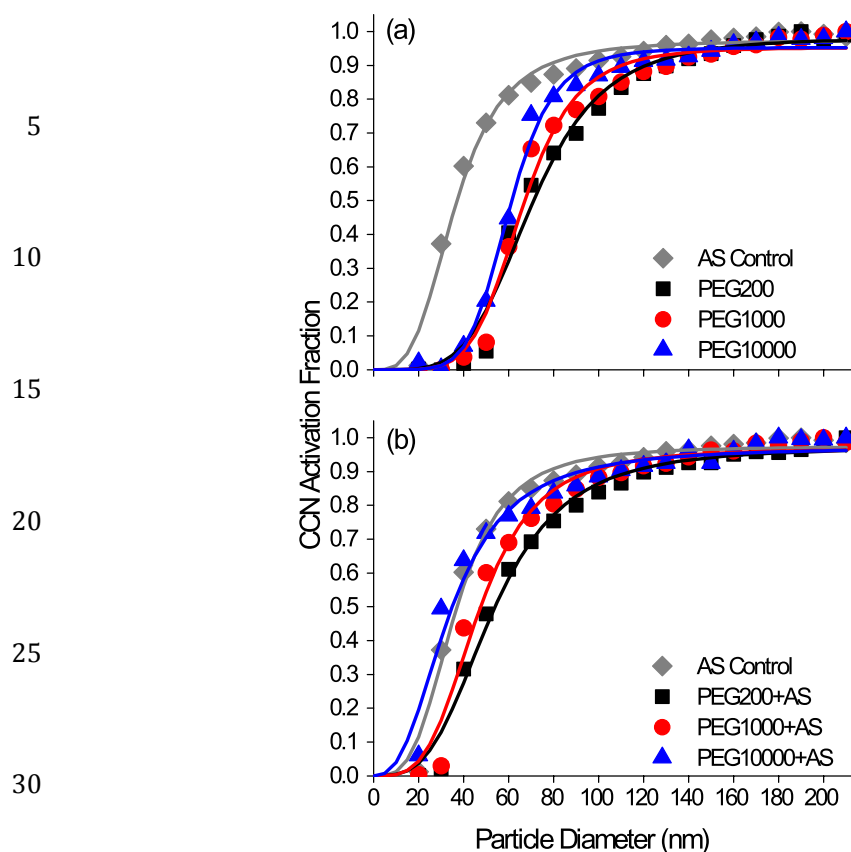
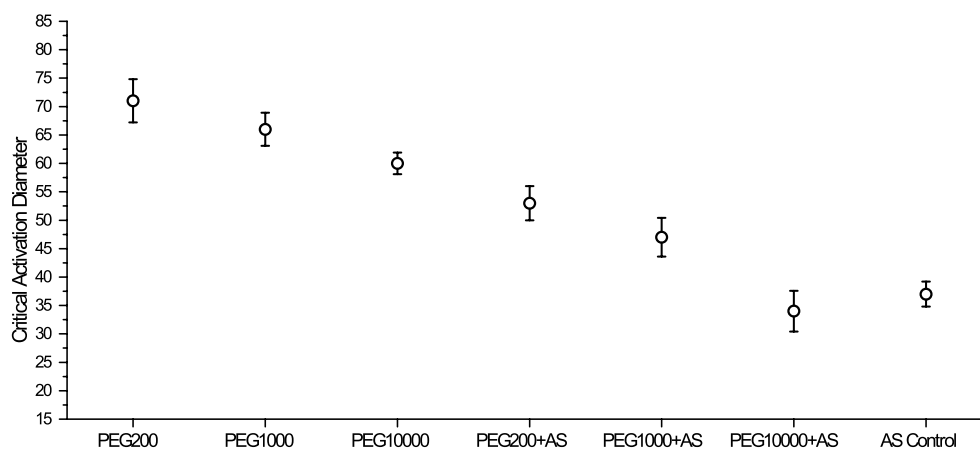


Figure 2. Measured cloud condensation nuclei (CCN) activation fraction as a function of particle size for (a) the PEG-containing aerosol systems and (b) the PEG-AS aerosol systems with PEG:AS mass ratios of 2:1. CCN activity was characterized based on the critical activation diameter at a water-supersaturation of 0.6%. Solid lines are the sigmoidal curve fit to the activation fraction measurements for each aerosol system. Critical diameter was characterized based on sigmoid inflection points. R-square values for the sigmoidal fits ranged between 0.95 and 0.99.



5 **Figure 3.** Measured values of D_{crit} for the PEG, PEG-AS and, AS Control aerosol systems. Values of D_{crit} were determined by fitting the activation-fraction measurements with sigmoidal curves, as shown in Figure 2. Circles indicate the diameter corresponding to the sigmoid inflection point, D_{crit} . Error bars indicate 95% confidence intervals of D_{crit} .

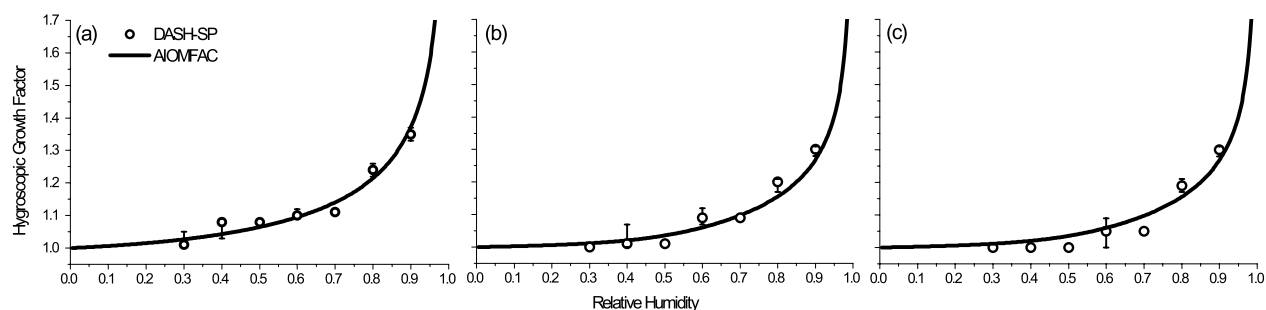


Figure 4. Comparison of hygroscopic growth factors measured with the DASH-SP and those predicted by AIOMFAC for (a) PEG200, (b) PEG1000, and (c) PEG10000 for particles with diameters of 250 nm. For the DASH-SP measurements, symbols indicate the average HGF and error bars indicate the maximum and minimum HGFs derived from repeat measurements.

5

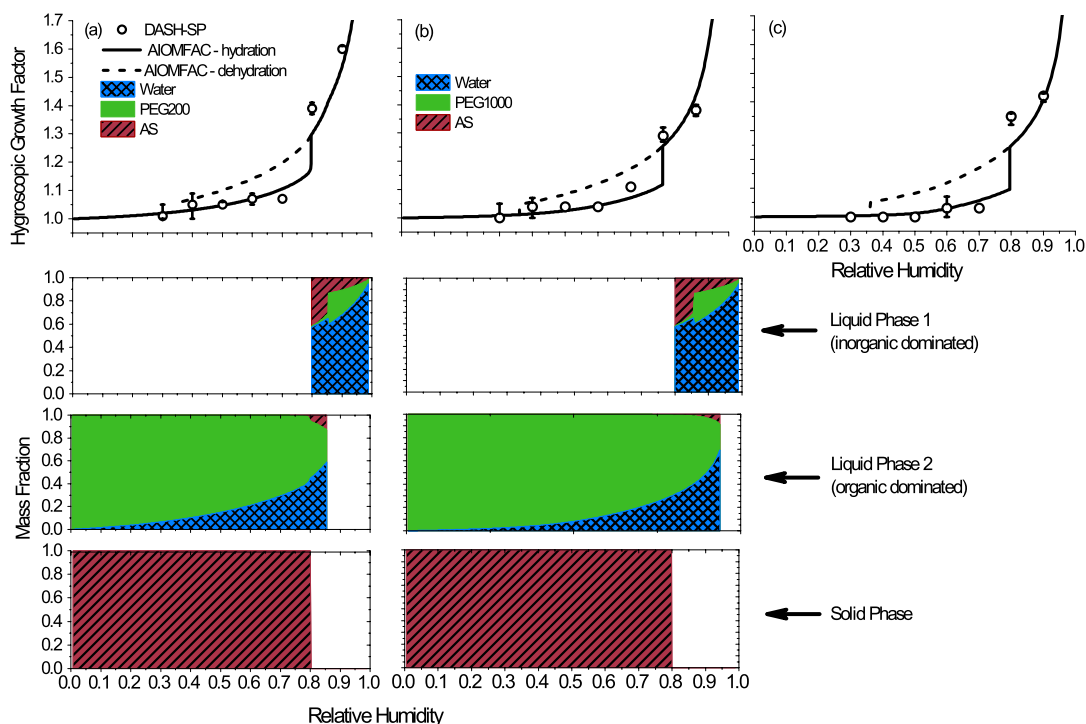
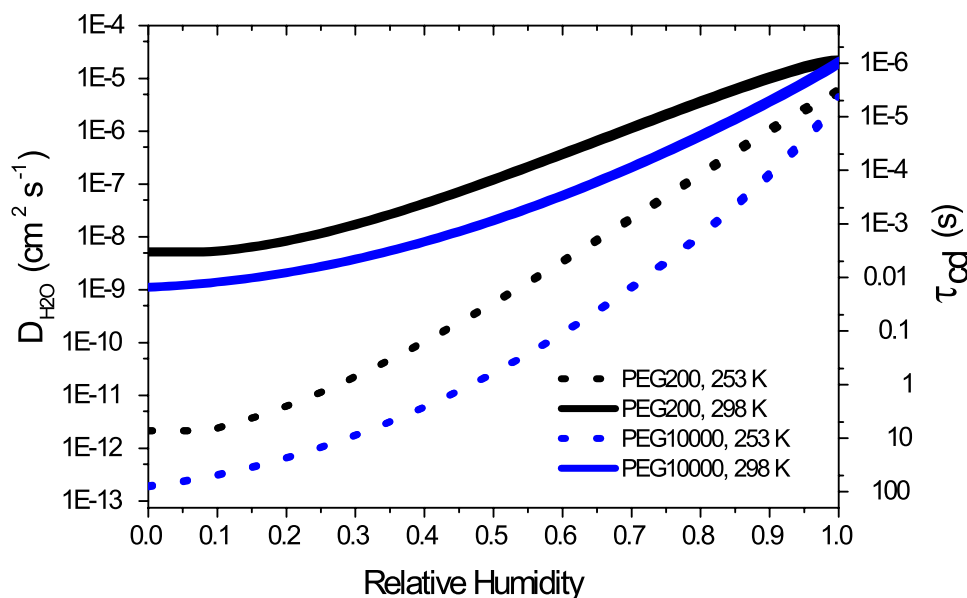


Figure 5. Top panels: Comparison of hygroscopic growth factors measured with the DASH-SP and those predicted by AIOMFAC for (a) PEG200-AS, (b) PEG1000-AS, and (c) PEG10000-AS for particles with diameters of 250 nm. For the DASH-SP measurements, symbols indicate the average HGF, and error bars indicate the maximum and minimum HGFs derived from repeat measurements. Panels below the growth curves show the AIOMFAC-predicted chemical composition of three potential phases present in the particles - an inorganic-dominated liquid phase, an organic-dominated liquid phase, and a solid phase - as a function of relative humidity. Further model refinements are needed before the detailed LLE phase behavior of aerosol systems containing high-molecular-mass PEG can be predicted reliably. However, all PEG-AS systems are expected to undergo liquid-liquid phase separation, with the RH at which the two separated phases merge to a single liquid phase increasing with increasing PEG molecular mass.



5 **Figure 6.** Predicted bulk diffusivity of water ($D_{\text{H}_2\text{O}}$) and characteristic equilibration timescale (τ_{cd}) as a
 function of relative humidity at 298 and 253 K. At 298 K, water diffusion is predicted to be rapid for both
 PEG200 and PEG10000, and equilibration is expected to be achieved in the 4 s residence time of the
 DASH-SP humidifiers. At 253 K, higher particle viscosity results in equilibration timescales that approach
 100 s.

10

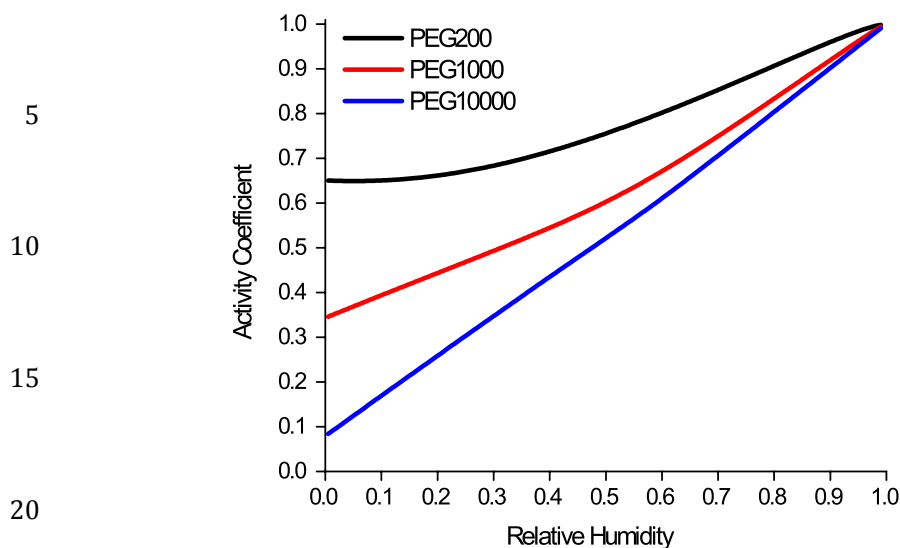


Figure 7. AIOMFAC predicted activity coefficients of water in PEG200, PEG1000, and PEG10000 as a function of RH. At low to moderate RH, activity coefficients are closer to unity in PEG200 as compared to the higher-molecular-mass PEG systems, indicating a lesser degree of thermodynamic non-ideality. Activity coefficients approach unity for all aerosol systems as RH approaches water saturation.

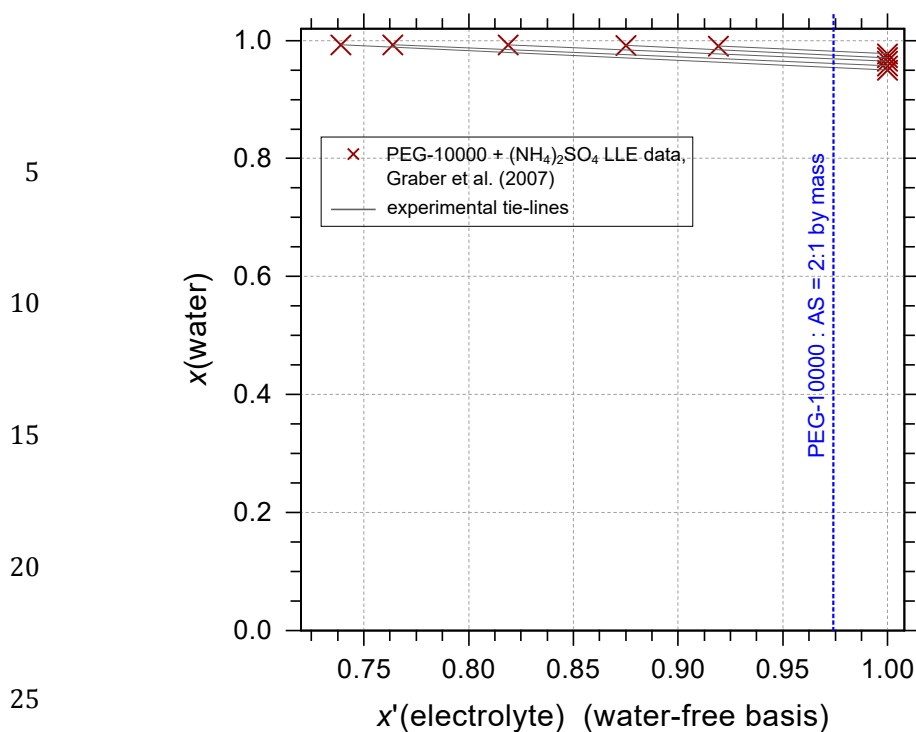


Figure A1. Experimental LLE tie-line data for the aqueous PEG10000-AS system at 298.15 K by Graber et al., (2007), shown as the mole fraction of water ($x(\text{water})$) in the ternary PEG10000-AS-water liquid bulk mixture versus the mole fraction of AS ($x'(\text{electrolyte})$) of the PEG10000-AS mixture on a water-free basis. The dashed blue line indicates the dry PEG10000:AS mass ratio of 2:1 studied in the DASH-SP experiments. Based on the observation of LLE at high mole fractions of water (relevant to high RH values), LLE is expected to persist from low RH to RH values exceeding those studied here with the DASH-SP for the PEG10000-AS aerosol system.